이학 석사 학위논문

Role of brain-infiltrating macrophages in collagenase-induced mouse intracerebral hemorrhage

콜라게나아제에 의한 마우스 뇌내출혈 모델에서 혈관으로부터 유입된 대식세포의 역할 규명

2015 년 2 월

서울대학교 대학원

협동과정 유전공학전공

장 용 호

Role of brain-infiltrating macrophages in collagenase-induced mouse intracerebral hemorrhage

지도교수 이 성 중

이 논문을 이학 석사 학위논문으로 제출함

2015 년 2 월

서울대학교 대학원
협동과정 유전공학전공
장 용 호

장용호의 이학 석사 학위논문을 인준함

2014 년 12 월

위 원 장 _____ (인)

부위원장 _____ (인)

위 원 _____ (인)

ABSTRACT

Role of brain-infiltrating macrophages in collagenase-induced mouse intracerebral hemorrhage

Yong Ho Jang

Interdisciplinary Graduate Program

in Genetic Engineering

The Graduate School

Seoul National University

Intracerebral hemorrhage (ICH) is one of the major causes of stroke, constituting 10% of all stroke cases. Upon ICH, the primary mechanical insult by increasing volume of hematoma is followed by massive infiltration of macrophages in the perihematoma regions. Recently, it has been reported that the function of macrophages is distinct depending on their activation type; M1, or classical activation, leads to pro-inflammatory responses, while M2, or alternative activation, contributes to tissue repair or healing. Since the function of brain-infiltrating macrophages after ICH has not been elucidated, I characterized the phenotype of macrophages infiltrating brain parenchyma and investigated their role in ICH.

Upon ICH injury, extravasated macrophage number increased in perihematomal region. To investigate the role of these brain-infiltrating macrophages, I depleted peripheral monocytes by i.p. clodronate liposome injection. In the monocytes-depleted mice, the ICH-induced neurological deficits were more severe compared to those of control mice, indicating a protective role of macrophages in ICH injury. The mRNA expression of Arginase-1 (an M2 marker) was upregulated in the ICH-injured brain, while iNOS (an M1 marker) expression was not significantly altered. In flow cytometry, mannose receptor (an M2 marker)-expressing macrophages increased at a delayed time point after ICH. The M2 polarization of the brain-infiltrating macrophages suggested that the brain microenvironment around macrophages may affect macrophage activation. To explore such possibility, bone marrow derived macrophages (BMDM) were co-cultured with mouse brain mixed glia cells (MBMG) and then tested for their activation phenotype. Upon co-culture with MBMG, the number of mannose receptor-positive BMDMs was significantly increased, which suggests that glia cells can induce macrophage M2 polarization. Furthermore, treatment with MBMG conditioned media increased the number of mannose receptor-expressing BMDM and the mRNA expression of Arg-1 and Ym1. Taken together, these data suggest that brain-infiltrating macrophages, after ICH, are differentiated to the M2 phenotype by brain glial cells, and thereby contribute to the recovery from ICH injury.

Key Words :

Intracerebral hemorrhage, stroke, macrophage, M2 polarizaiotn, BMDM, Glia, clodronate liposome

Student Number: 2012-23008

CONTENTS

Ⅰ. Introduction

Intracerebral hemorrhage (ICH) is a type of stroke, which occurs when a blood vessel within the brain ruptures allowing blood to leak into the brain parenchyma. It accounts for about 10% of all stroke cases and results from a wide spectrum of disorders (Mayer and Rincon, 2005). Although it occurs fewer, it is more likely to result in death or major disability than other strokes. However there is no effective treatment for ICH, since therapies are limited (Mayer and Rincon, 2005). Although significant studies on ICH are increasing, still studies are needed to develop specific and novel therapy for ICH.

In the central nervous system (CNS), microglia functions as an innate immune cells. Increasing evidence suggests that microglial activation may aggravate ICH-induced brain injury in mouse (Aronowski and Hall, 2005; Wang and Tsirka, 2005; Gao et al., 2008). Meanwhile, Neutrophil infiltrated into brain lesion contribute to ICH damage by producing reactive oxygen species, releasing proinflammatory mediators, and increasing permeability of BBB (Nguyen et al., 2007; Wang and Dore, 2007; Joice et al., 2009). In addition, macrophages accumulate at the lesion in ICH-induced mice brain (Hammond et al., 2012). Because inflammation plays a key role in secondary damage of ICH, the research about brain-infiltrating immune cells in ICH may be important to treat for ICH. Recently, a study using $CCR2^{-/-}$ mice suggest that these brain-infiltrating inflammatory monocytes may aggravate ICH in early time (Hammond et al., 2014). However, the inforrmation regarding brain-infiltrating macrophages in ICH still has been lacked.

Microglia/macrophages display remarkable plasticity and can change their phenotypes and exhibit different function in response to environment (Kigerl et al., 2009; Perry et al., 2010). In vitro, stimulation with lipopolysacharide and interferon-γ promote differentiation of "classically activated" M1 macrophages that produce and release proinflammatory mediators (Ding et al., 1988). Conversely, interleukin (IL)-4 and IL-10 induce differentiatiom of "alternatively activated" M2 macrophages that promote angiogenesis and matrix remodeling (Sica et al., 2006). Whereas in murine ischemic stroke model, polarization dynamics of microglia/macrophages has been characterized, in ICH model, macrophage polarization has not been addressed yet (Hu et al., 2012). In this study, I used a mouse model of collagenase-induced ICH to explore the function and phenotype of brain-infiltrating macrophage after hemorrhagic stroke. I found that the macrophages infiltrated into the brain parenchyma after hemorrhage contribute to recovery from ICH by M2 polarization at a delayed time.

Ⅱ. Material and Method

Animals

Cx3cr1$^{+/GFP}$ mice with sequence encoding GFP knocked into the gene encoding the CX3CR1 were from the Jackson Laboratory. 7-11 week old C57BL/6 mice were purchased from Daehan Bio Link. All mice were housed at 23 ± 2℃ with a 12 h light-dark cycle and fed food and water *ad libitum*. All surgical and experimental procedures were reviewed and approved by the Institutional Animal Care and Use Committee at Seoul National University.

ICH model

The procedure for inducing ICH by collagenase injection in mice was adapted from a protocol previously described (Wang and Dore, 2007). Briefly, WT and *Cx3cr1*$^{+/GFP}$ mice (8-12 week old males, 22-25 g) were anesthetized using Avertin (250 mg/kg body weight, i.p.), and placed on a stereotaxic apparatus (myNeuroLab, St. Louis, MO, USA). Animals were injected with PBS or collagenase VII-S (0.075 U in 0.5 µl PBS; Sigma, St. Louis, MO, USA) at a rate of 0.2 µl/min into the right caudate putamen (stereotaxic coordinates in millimeters with reference to bregma: AP, -0.9; ML, +2.8; DV, -4.0) using a 26 G needle. After 5 min, the needle was removed in three intermediate steps for 3 min to minimize backflow. The incision was disinfected with povidone iodide solution, sutured, and the animals were kept on a warm pad during recovery.

Injury volume analysis

To prepare brain tissue sections, animals were deeply anesthetized with urethane and perfused intracardially with saline followed by cold 4% paraformaldehyde (PFA) in a 0.1 M phosphate buffer. The brains were removed, post-fixed overnight in the same fixative at 4℃, rinsed twice with PBS, and placed in 10, 20, and 30% sucrose in PBS, serially, for 72 h at 4℃. The brains were then quickly frozen and cut into serial coronal sections (50 μm thickness) in a cryostat (CM3050S, Leica, Germany). Sections were collected as free-floating sections in cold PBS and then used for histological analysis. Five coronal brain slices from different levels of the injured hemorrhagic area were selected from each mouse brain and used for cresyl violet staining. The injury area was quantified using Image J software (National Institutues of Health, Bethesda, MD, USA), and the injury volume was calculated in cubic millimeters (mm^3) by multiplying the section thickness by the measured injury areas as described.

Behavioral test

Adhesive removal test (ART) was performed as described previously (Bouet, 2009). Mice were habituated at least 30 min prior to applying the sticky tape on the sole of fore left paw. The removal time is defined as from the point that the mouse reacts to the presence of the adhesive tape strips to detach the tape using its mouth or fore limb. The timing of the procedure to test one mouse is 300 seconds maximum. ART was performed at 1 day and 3 days after ICH or sham operation.

Neurological function was measured by scoring the focal deficit with use of a 28-point neurological scoring system (Clark, 1998). Habituated mice were scored as following subjects: (1) Body symmetry, (2) Gait, (3) Climbing, (4) Circling behavior

(5) Front limb symmetry (6) Compulsory circling (7) Whisker response. 1, 3 days after ICH, scoring was performed as 0 - 4 per a subject and the scores were averaged.

Peripheral macrophages/monocytes depletion

Peripheral monocytes/macrophages were systemically depleted using clodronate liposome suspension (ClodronateLiposome.com, Amstherdam, Nederland). Mice were injected intraperitoneally with 1 mg of clodronate liposome (Cl_2MDP) or saline 1 day before ICH surgery. After 1 day ICH, an additionally injection has given to the mice for increasing the depletion rate. The depletion efficiency was evaluated by anti CD68 immunofluorescence staining on the slices of the spleen from the mice.

Immunohistochemistry

Immunostaining was carried out using previously established protocols (Cho et al., 2008). The sections were incubated in a blocking solution (5% normal donkey serum, 2% BSA, and 0.1% Triton X-100) for 1 h at room temperature (RT). The sections were then incubated overnight at 4℃ with the following antibodies: goat anti-arginase-1 (1:50; Santa Cruz Biotechnology, CA, USA), rat anti-CD68 (1:100, AbD Serotec, Oxford, UK). The sections were incubated for 1 h at RT with Cy3-conjugated secondary antibodies (1:200; Jackson ImmunoResearch, West Grove, PA, USA), and then mounted on gelatin-coated slides and coverslipped with VectaShield medium (Vector Labs, Burlingame, CA, USA). All images were acquired by using confocal laser scanning microscopy (LSM700; Carl Zeiss, Germany).

Quantitative real-time RT-PCR

The cDNA was synthesized using total RNA from mouse brain tissue or in vitro cultured cell. The reverse transcription mixture was consist of 1~3 ug of total RNA, oligo-dT, M-MLV, RNAse inhibitor, DTT, RT buffer and then synthesized at 37℃ for 1 hour. Real-time RT-PCR was performed using SYBR Green PCR Master Mix (ABI, Warrington, UK) as described previously (Cho et al., 2008). Reactions were performed in duplicate in a total volume of 12 μl containing 10 pM primer, 5 μl cDNA, and 6 μl SYBR Green PCR Master Mix (Applied bio). The mRNA levels of each target gene were normalized to that of GAPDH mRNA. Fold-induction was calculated using the $2^{-\Delta\Delta CT}$ method, as previously described (Livak and Schmittgen, 2001). All real-time RT-PCR experiments were performed at least three times, and are presented as mean ± SEM unless otherwise noted. The following sequences of primers were used for real-time RT-PCR: Arginase-1 forward: 5'-GGG CTC TGA TGA GAA GGA GA-3'; Arginase-1 reverse: 5'-GTA GAT GCC ACG CTG GTA CA-3'; Chi3L3 (Ym1) forward: 5'-GAA GGA GCC ACT GAG GTC TG-3'; Chi3L3 (Ym1) reverse: 5'-CAC GGC ACC TCC TAA ATT GT-3'; iNOS forward: 5'-GGC AAA CCC AAG GTC TAC GTT-3'; iNOS reverse: 5'-TCG CTC AAG TTC AGC TTG GT-3'; TNF-α forward: 5'-AGC AAA CCA CCA AGT GGA GGA-3'; TNF-α reverse: 5'-GCT GGC ACC ACT AGT TGG TTG T-3'.

Primary mouse brain glial cell culture

Primary mouse brain mixed glial cultures were prepared as previously described (Lee et al., 2000). Briefly, mixed glial cultures were prepared from postnatal day 1-3 wild type (WT) mice. After removing meninges from the cerebral hemisphere, tissue was dissociated into a single-cell suspension by gentle repetitive pipetting. Cells were cultured in Dulbescco's Modified Eagle's medium (DMEM) supplemented with

10 mM HEPES, 10% FBS, 2 mM L-glutamine, 1X NEAA and 1X antibiotic/antimycotic in 75 cm^2 flasks at 37℃ in a 5% CO_2 incubator, and the medium was changed every 5 days.

Primary mouse bone marrow-derived macrophage culture

The protocol of bone marrow-derived macrophage cultures and cryopreservation were adapted from a protocol described previously (Marim et al., 2010). Briefly, femurs and tibias were obtained from 8-12 week old C57BL/6 mice or *Cx3cr1*$^{+/GFP}$ mice. The bones were flushed with a syringe filled with DMEM to extrude bone marrow into a 50 ml sterile tube. The cells were gently homogenized using plastic pipette and aliquoted in freezing media containing 90% fetal bovine serum and 10% DMSO. The aliquots were maintained in a -80℃ for 24 hours and then transferred to a liquid nitrogen tank. Bone marrow cells were thawed and washed with warm-DMEM and then cultured in DMEM supplemented with 10mM HEPES, 10% FBS, 2mM L-glutamine, 1X NEAA, 1X antibiotic/antimycotic and 30 ng/ml recombinant human M-CSF (rhM-CSF, Peprotech, Rocky Hill, NJ, USA) at 37℃ in a 5% CO_2 atmosphere for 5 days. For mRNA quantification or flow cytometry analysis, BMDMs were seeded in a 6-well plate (2.5 ~ 5 x 10^5/well) with growth media supplemented with 10 ng/ml recombinant human M-CSF for 2 days.

Co-culture experiment

While the BMDM were removed from the plate by scrapper, the MBMG were detached by trypsin simultaneously. Cells were counted using a hemocytometer (2.5 ~ 5 x 10^5 cells) and then added to a 60 ø culture dish at a 1:1 ratio in BMDM growth

medium containing 10 ng/ml rhM-CSF. Co-cultures were incubated at 37℃ in a CO_2 incubator.

MBMG conditioned media treatment

Two weeks after MBMG culture, conditioned media were collected. To prevent cell contamination, conditioned media were centrifuged shortly and then stored at -80℃ deepfreezer. A 1:1 mixture of MBMG conditioned media and BMDM growth media was used for treatment.

Flow cytometry

The mice were deeply anesthetized by urethane and intracardially perfused with ice-cold saline. Ipsilateral hemispheres were trimmed the anterior and posterior side from the needle hole, and then residues of brain hemispheres were homogenized mechanically to a single cell-suspesnsion. Co-cultures or BMDMs were removed from the plates with cold PBS and resuspended using a pipette. Cells were washed with ice-cold 2% fetal bovine serum (FBS) in PBS, and incubated with Fc Blocker™ (BD Bioscience, San Jose, CA) for 10min at 4℃ prior to staining with CD11b-FITC, CD45-PE, CD206-APC, F4/80-PE/Cy7 (Biolegend Inc, San Diego, CA). BD FACSCalibur flow cytometer (BD Bioscience) was used to measure the microglia as $CD11b^{+}CD45^{med}$, peripheral macrophage as $CD11b^{+}CD45^{high}$, BMDM as $CD45^{+}GFP^{+}$ or $CD11b^{+}CD45^{+}$. Data were acquired with analyzed with BD CellQuest™system (BD Biosciences).

Statistical analysis

Statistically differences between two groups were determined by two tailed Student's *t*-test. Differences among multiple groups were made using one-way ANOVA followed by Bonferroni correction. All data are presented as the mean ± SEM, and differences were considered significant when the P value was less than 0.05

Ⅲ. RESULT

Macrophages accumulate in the perihematomal region after ICH

To test ICH imjury triggers macrophage infiltration in brain parenchyma, I performed collagenase induced ICH with *CX3CR1*$^{+/GFP}$ mice which express GFP in macrophage or microglia. (Fig. 1). Following ICH, CX3CR1^{+} cells were increased in the perihematomal region. Especially 3 days after ICH, round-shape CX3CR1^{+} cells, presumably activated microglia or macrophage appeared around the perihematomal region that were further accumulated on day 7 (Fig. 1C). To quantify the brain-infiltrating macrophages after ICH, ipsilateral brain tissue from injured wild type mice was measured by flow cytometry. Consistent with previous studies, microglia population (F4/80^{+}CD45^{med}) and macrophage population (F4/80^{+}CD45^{high}) increased for 7 days after ICH (Fig. 1E).

Peripheral monocytes depletion attenuates the recovery from ICH at a delayed time

Because macrophages infiltration was increased in ipsilateral mice brain after ICH, I next determined the contribution of these cells to ICH by depleting monocytes/macrophages. For this purpose, I used clodronate liposome (Cl_2MDP) that is designed to kill a phagocytic immune cells. Mice were treated with Cl_2MDP via i.p. injection 1 day before ICH and again 1 day after ICH (Fig. 1A). The efficiency of monocyte depletion was confirmed by immonostaining monocytes (CD68) in spleen

sections (Fig.2 B). Cresyl violet staining of ipsilateral brain sections from Cl_2MDP- or saline-treated mice after ICH show that monocyte/macrophage-depleted mice have enlarged infarct volume after ICH compared to control mice (Fig. 2C and 2D). Consistent with the histologic data, the mice treated with Cl_2MDP displayed less severe sensory-motor function (Fig. 2E) and focal deficits (Fig. 2F) than control mice at day 3. These findings indicate that the brain-infiltrating macrophages play protective role in ICH at 3 days.

M2 marker expression is induced in injured brain after ICH

To elucidate mechanisms underlying the neuroprotective role, I characterized the polarization aspect of these brain-infiltrating macrophages following ICH. Arg-1 (M2) mRNA expression was upregulated in the ipsilateral ICH brains while iNOS (M1) transcript level was not significantly altered for 7 days after ICH (Fig. 3A). Consistent with the mRNA expression levels, Arg-1 immunoreactivity was enhanced in microglia or macrophage at 3 days. Furthermore, Arg-$1^{+}$$GFP^{-}$ cells were also detected, which means CX3CR1 negative cells also express Arg-1 on hemorrhagic site at perihematomal site 3 days after ICH (Fig. 3B). To further investigate the activation phenotype of microglia and macrophage in ICH injured mice brain, WT mice were subjected to ICH and the cells from their ipsilateral brain were measured by flow cytometry. The percentages of mannose receptor (CD206)-expressing macrophage population ($CD11b^{+}CD45^{high}$) increased to 68% 7 days post-ICH, whereas $CD206^{+}$ microglia population ($CD11b^{+}CD45^{med}$) increased to 16% (Fig. 4). This finding suggested that the majority of macrophages were activated toward M2 phenotype once they infiltrated into brain after ICH.

Glial cells induce macrophage M2 polarization in vitro

Since brain-infiltrating macrophage polarized to M2, I tested if brain glial cells affect macrophage M2 polarization. A previous study showed that BMDM exhibit M2 like phenotype after co-culture with astroglioma cell line (Ponomarev et al., 2010). To determine whether the glial cells activate the macrophage toward M2 directly, bone marrow derived macrophages (BMDM) were co-cultured with primary cultured mouse brain mixed glia (MBMG) for 1 day or 3 days. BMDM from *Cx3cr1*$^{+/gfp}$ mice were used to distinguish between BMDM and microglia from MBMG. The percentages of CD206^{+} cells in BMDM population (GFP^{+}CD45^{+}) increased to 20% at 3 days after co-culture with MBMG (Fig. 5). To test whether MBMG induce an M2 polarization via soluble factor or direct cell to cell interaction, I collected conditioned media of primary cultured MBMG, and then treated the MBMG conditioned media to BMDM for 1 day or 3 days. Then, mRNA expression of M1 or M2 marker genes in the BMDM was measured by real-time RT-PCR. After 3 days, the mRNA expression of Arg-1 and Ym-1in BMDM increased by 1.5 and 6 folds, respectively (Fig. 6A and 6B). However iNOS and TNF-α mRNA expressions, M1 marker genes, were not significantly upregulated after MBMG conditioned media treatment (Fig. 6C and 6D). Additionally, an M2 specific protein expression was analyzed by flow cytometry. The number of CD206^{+} BMDM was increased at 1 day and 3 days after MBMG conditioned media treatment (Fig. 6E).

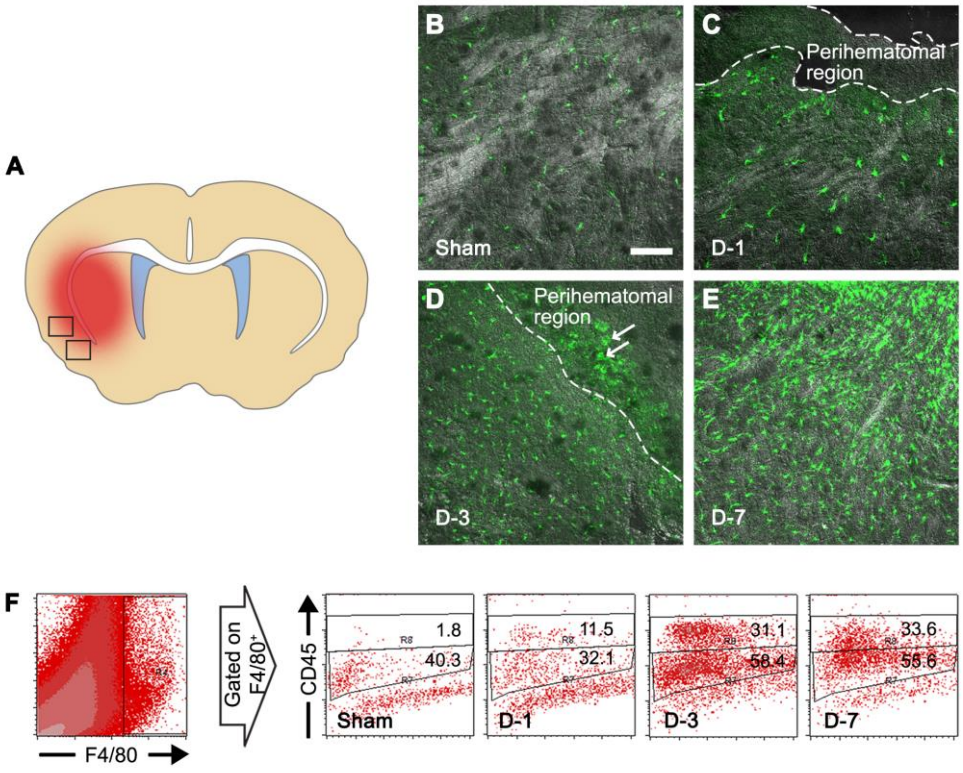
A
B
Sham
C
Perihematomal region
D-1
D
Perihematomal region
D-3
E
D-7
F
F4/80
Gated on F4/80+
CD45
1.8
40.3
Sham
11.5
32.1
D-1
31.1
58.4
D-3
33.6
55.6
D-7

Fig.1. CX3CR1^{+} cells increase at the perihematoma after ICH

(A) Perihematomal regions were taken from hemorrhagic brain section for observation of CX3CR1^{+} cells. **(B-E)** Representative images on brain sections were obtained from *Cx3cr1*$^{+/GFP}$ mice at 1, 3 and 7 days after ICH or sham operated. 3 days after ICH, amoeboid form cells were detected at the perihematoma site (arrows). Confocal microscopic images are representative of three independent experiments (Scale bar, 100 μm). **(F)** Representative dot plots were acquired from ICH induced ipsilateral brain by flow cytometry. Microglia and macrophages were defined as F4/80^{+}CD45^{med} and F4/80^{+}CD45^{high} respectively. The flow cytometry data are representative of three independent experiments.

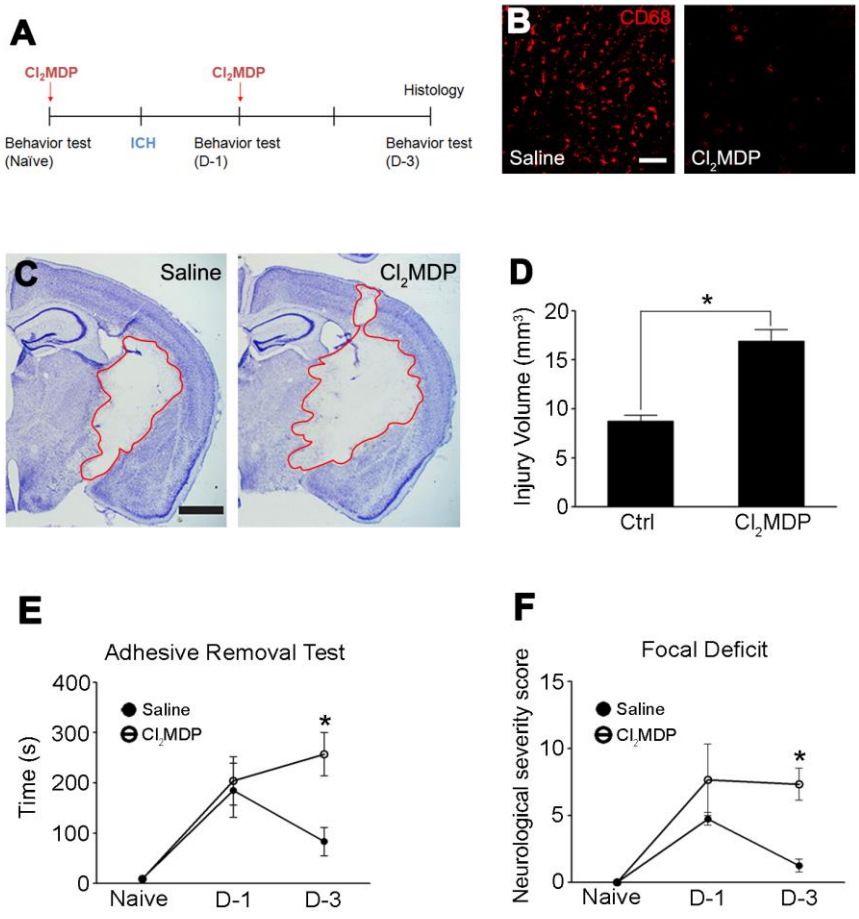
A
Cl2MDP
Cl2MDP
Histology
Behavior test (Naïve)
ICH
Behavior test (D-1)
Behavior test (D-3)
B
CD68
Saline
Cl2MDP
C
Saline
Cl2MDP
D
Injury Volume (mm3)
20
15
10
5
0
*
Ctrl
Cl2MDP
E
Adhesive Removal Test
Time (s)
400
300
200
100
0
Saline
Cl2MDP
*
Naive
D-1
D-3
F
Focal Deficit
Neurological severity score
15
10
5
0
Saline
Cl2MDP
*
Naive
D-1
D-3

Fig.2. Elimination of peripheral monocytes attenuates the recovery from ICH

(A) Schematic diagram of the depletion protocols. **(B)** Spleen sections were obtained from Cl_2MDP received ICH mice and stained with anti CD68 antibody. The immunostaining images are representative of three independent experiments (Scale bar, 50 μm). **(C)** 1 day after Cl_2MDP injection, mice were subjected to ICH, and the brains were sectioned and stained with cresyl violet at 3 days following collagenase injection. Representative pictures are shown (Scale bar, 1 mm). **(D)** Quantification of hemorrhagic injured volume was shown in a graph (n=4/group, *P< 0.05). **(E, F)** 1 day after Cl_2MDP or saline ip. Injection, mice were subjected to ICH and neurological severities were evaluated by focal deficit and sticky tape remove time at 1 and 3 days after ICH (n=6 for naïve group, n=5 for D-1 group, n=5 for D-3 group in ART; n=4 for saline group, n=3 for Cl_2MDP group in focal deficit, *P< 0.05). Data are expressed as mean ± SEM.

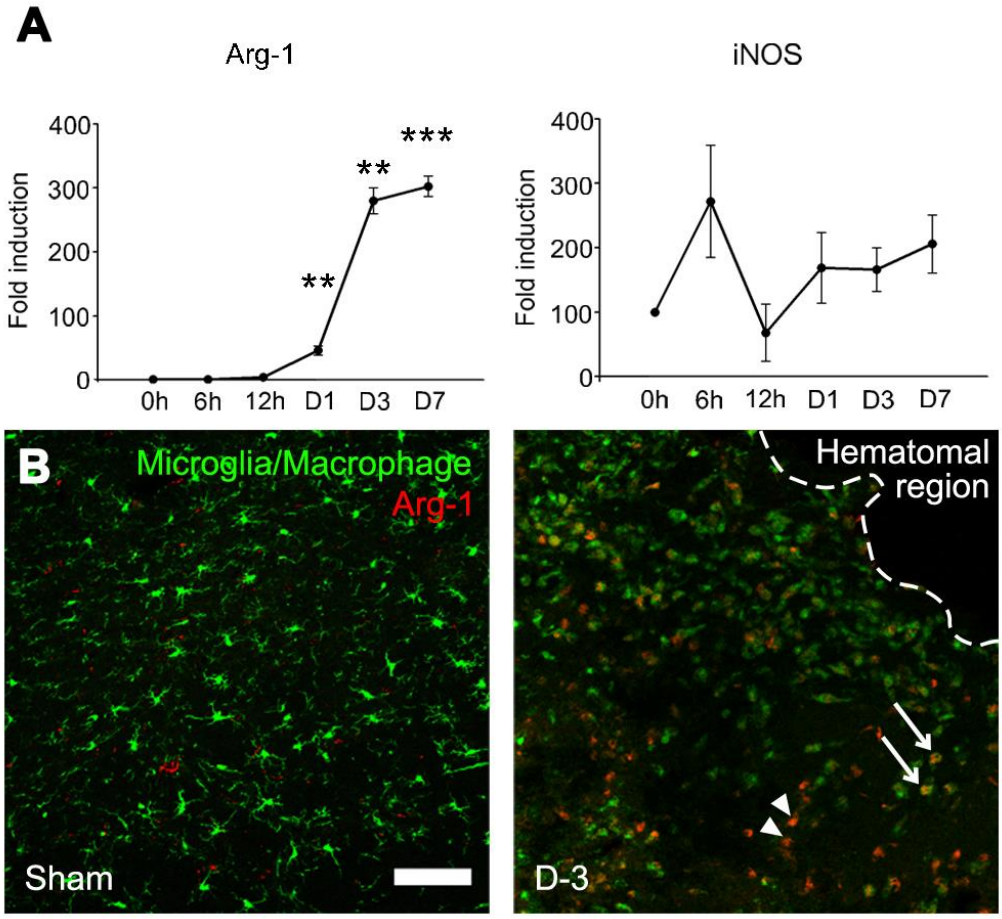
A
Arg-1
iNOS
Fold induction
400
300
200
100
0
0h
6h
12h
D1
D3
D7
**
**
***
B
Microglia/Macrophage
Arg-1
Sham
Hematomal
region
D-3

Fig.3. M2 marophages are increased in the ipsilateral of mice brain after ICH.

(A) Arg-1 and iNOS mRNA expressions in the ICH mice brain were measured by real-time RT-PCT. Total RNA was isolated from ipsilateral hemorrhagic tissue and used for quantitative real-time RT-PCR (n=3/group, **P< 0.01, ***P< 0.001). **(B)** Representative images of immunofluorescence of Arg-1 on the *CX3CR1*$^{+/GFP}$ mice brain sections were obtained at 3 days after ICH or sham operated. Arg-1 immunofluorescences were merged with GFP signal (arrow) or not (arrow head). The immunofluorescence images are representative of two independent experiments (Scale bar, 100 μm).

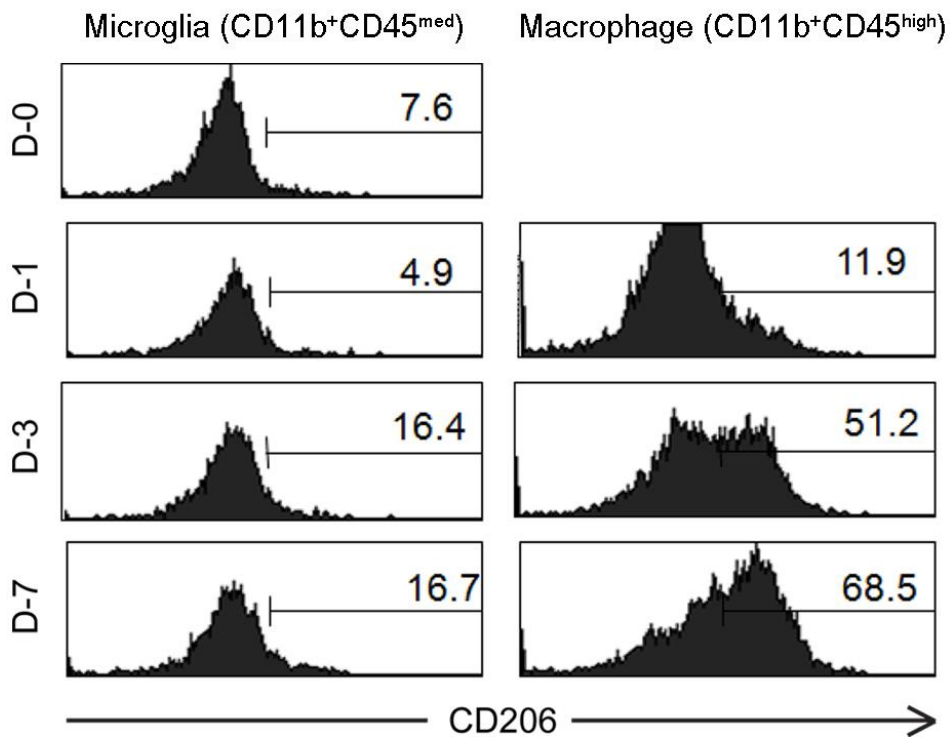
Microglia (CD11b+CD45med)
Macrophage (CD11b+CD45high)
D-0
D-1
D-3
D-7
7.6
4.9
11.9
16.4
51.2
16.7
68.5
CD206

Fig.4. Alternatively activated infiltrating macrophages increased in the ICH-injured brain.

The cells from the injured tissue were obtained 1, 3 and 7 days after ICH injury and stained with anti CD11b-FITC, CD45-PE and CD206-APC antibodies. Representative flow cytometry histogram shows $CD206^{+}$ cells gated on $CD11b^{+}CD45^{+}$ populations. Microglia and macrophages were defined as $CD11b^{+}CD45^{med}$ and $CD11b^{+}CD45^{high}$ respectively. The flow cytometry data are representative of three independent experiments.

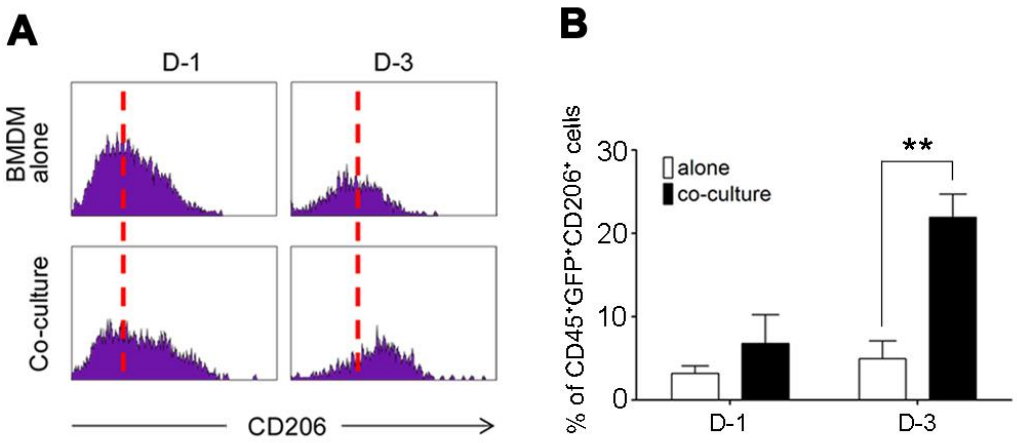
A
D-1
D-3
BMDM alone
Co-culture
CD206
B
% of CD45+GFP+CD206+ cells
alone
co-culture
**
30
20
10
0
D-1
D-3

Fig.5. Co-culture with MBMG affects BMDM to polarize toward M2

(A) BMDM from *Cx3cr1*$^{+/GFP}$ mice were cultured with or without MBMG from wild type C57BL/6 mice at 1:1 ratio for 1day or 3days. The cells were stained with anti CD45-PE and CD206-APC antibodies (left). Representative histograms of CD206 expression were gated on $GFP^{+}CD45^{+}$ populations (right). **(B)** Quantification of percentages of $CD206^{+}$ populations in BMDM was calculated by flow cytometry (n=3/group, *P< 0.05). Data are presented as means±SEM.

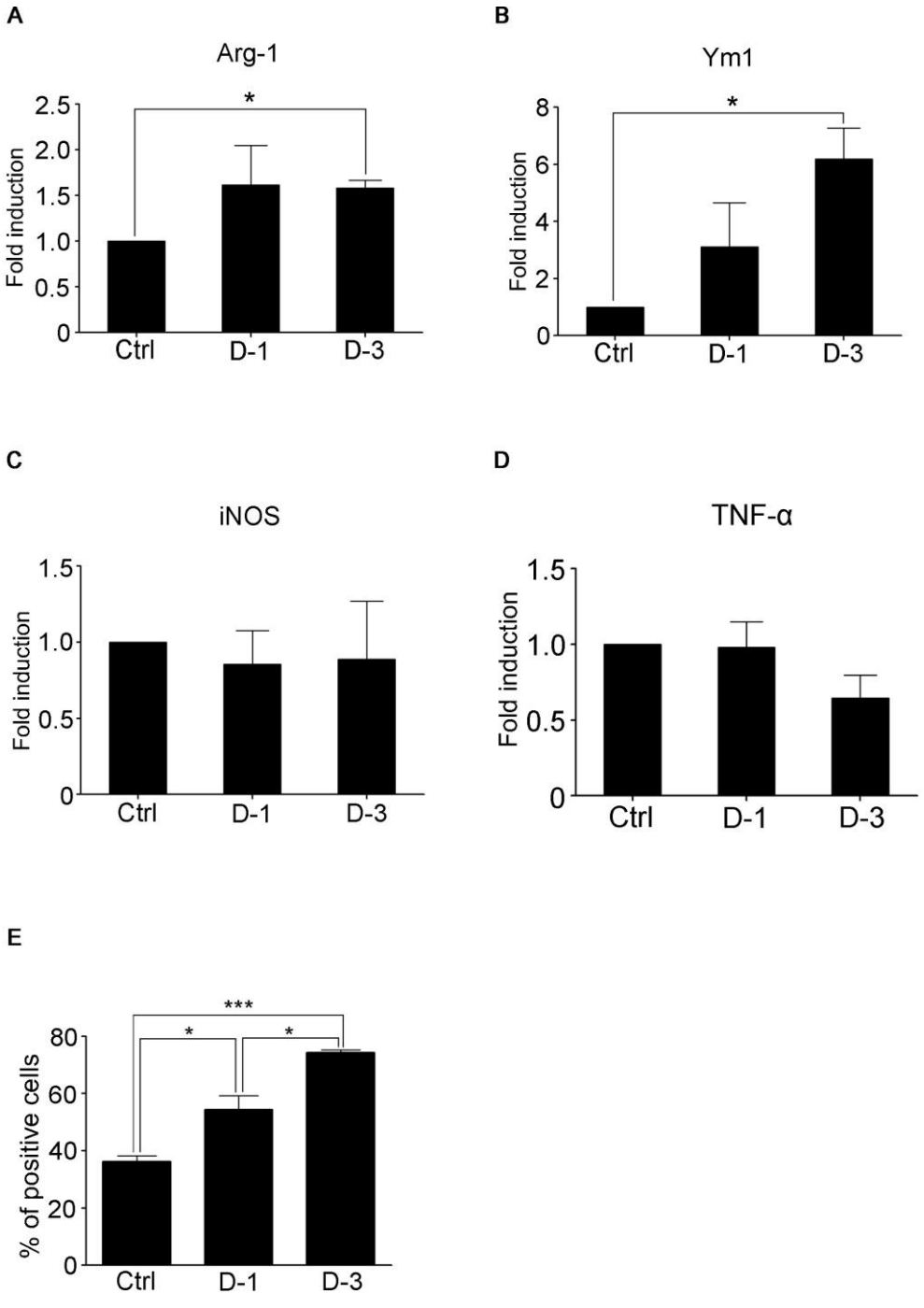
A
Arg-1
Fold induction
2.5
2.0
1.5
1.0
0.5
0
*
Ctrl
D-1
D-3
B
Ym1
Fold induction
8
6
4
2
0
*
Ctrl
D-1
D-3
C
iNOS
Fold induction
1.5
1.0
0.5
0
Ctrl
D-1
D-3
D
TNF-α
Fold induction
1.5
1.0
0.5
0
Ctrl
D-1
D-3
E
% of positive cells
80
60
40
20
0
***
*
*
Ctrl
D-1
D-3

Fig.6. Soluble factors from MBMG effect upregulation of M2 polarization in BMDM

(A-D) Total RNA was isolated from BMDM at 1day or 3days after MBMG conditioned media treatment. Arg-1, Ym1, iNOS, and TNF-α mRNA expressions were measured by real-time RT-PCR (n=3/group for Arg-1, n=5/group for Ym1, n=3/group for iNOS, n=3/group for TNF-α, *P< 0.05). **(E)** Quantification of $CD206^+$ cells from BMDM was analyzed by flow cytometry. BMDM were treated MBMG conditioned media for 1 day and 3 days. The cells were harvested and stained with CD45-PE, CD11b-FITC and CD206-APC. The percentage of $CD206^+$ cells were calculated from $CD45^+CD11b^+$ populations (n=3/group, *P< 0.05, ***P< 0.001). Data are expressed as means±SEM.

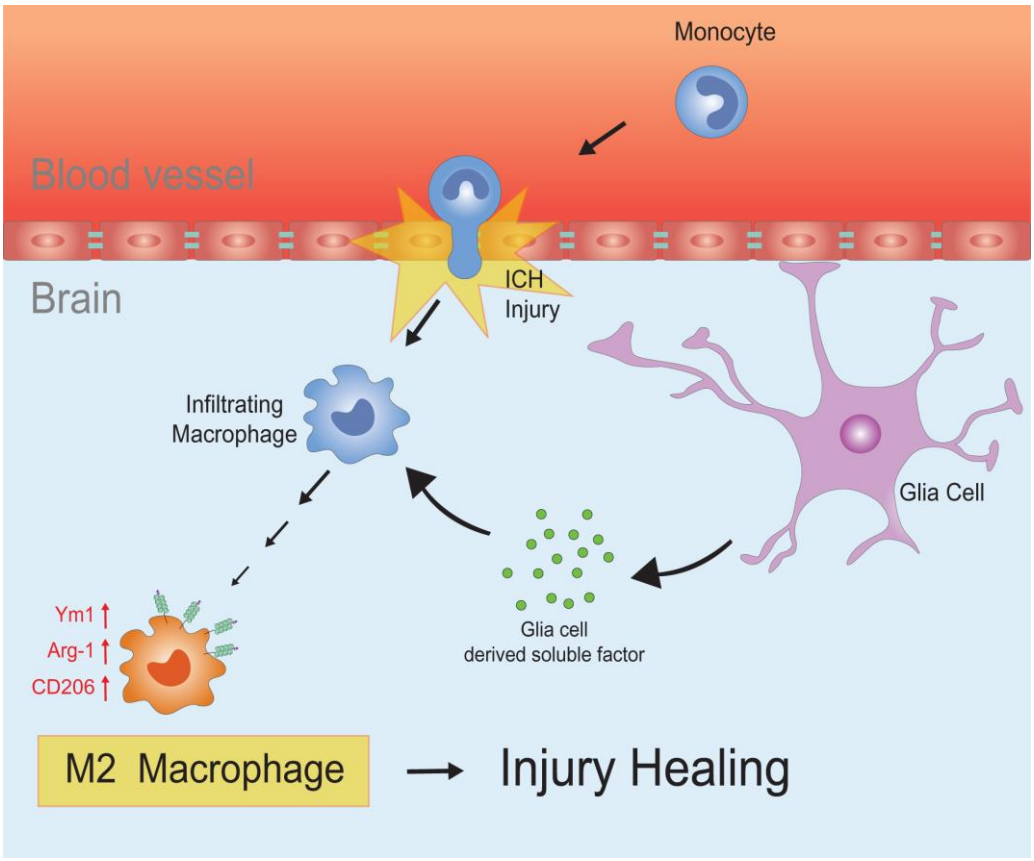
Monocyte
Blood vessel
Brain
ICH
Injury
Infiltrating
Macrophage
Glia Cell
Ym1
Arg-1
CD206
Glia cell
derived soluble factor
M2 Macrophage
Injury Healing

Fig.7. Summary

Peripheral blood-derived monocytes are recruited when ICH occur, then infiltrating macrophages are exposed by surrounding microenvironment of brain. The macrophage may contact factors from glial cells in the brain at first time. The factors from glial cells activate infiltrating macrophage toward M2 phenotype. As previous reports, M2 macrophages are involved with neuroprotection and repair after injury. Therefore, infiltrating macrophages driven toward M2 by glial cells facilitate recovery from collagenase-induced ICH.

Ⅳ. Discussion

Comparing with ischemic stroke model, researches focused on microglia / macrophages in hemorrhagic stroke have been lacked. A recent study showed that Gr1+ inflammatory macrophage and dendritic cells were the majority of infiltrating leukocytes 12 hours after ICH (Hammond et al., 2012). Another study demonstrated that inflammatory monocytes were recruited and exacerbate disability following ICH in early time (Hammond et al., 2014). These studies focused on the inflammatory phenotypes and functions of infiltrating macrophages after acute ICH. However, peripheral monocytes were also detected at later time after ICH (Hammond et al., 2014) and infiltrating macrophages play an anti-inflammatory role in recovery from spinal cord injury (Shechter et al., 2009). Here, I show the peripheral monocytes were required for recovery from ICH at D-3 (Fig. 2). This finding suggests that although infiltrating macrophages aggravate the ICH in early time, they may improve the ICH in a delayed time.

Macrophages are highly plastic cells that display different phenotypes, proinflammatory or anti-inflammatory, in response to specific microenvironment. Accordingly, macrophage polarization toward different phenotype at different stages of injury might account for this dual role (Hu et al., 2014). As this property, macrophage is double-edged sword in diverse disease progression. Microglia also have a plasticity that can change their phenotypes at the injury in CNS. Microglia and macrophage were reported as the potent modulator of brain repair (Hanisch and Kettenmann, 2007; Miron et al., 2013). On the other hand, they exacerbate the damages in CNS disease (Ekdahl et al., 2003; Liu et al., 2007). In a recent study, M2 phenotype was upregulated in early time after MCAO-induced stroke model and subsided with time, while M1

phenotype increase over time after ischemic stroke (Hu et al., 2012). However, polarization of macrophage in mouse hemorrhagic stroke model was not addressed yet. In current study, macrophage polarization in a hemorrhagic mice brain was measured with mRNA expression level of M1 or M2 markers. Arg-1 mRNA expression was increased over time after ICH, while iNOS was not changed significantly (Fig. 3). Although I conclude that the tendency of polarization in mice brain after ICH is towardM2 due to the results of Arg-1 and Ym1 mRNA expression, the possibility of temporary M1 marker upregulation still remains. Because the stauts of microglia and macrophage polarization *in vivo* is too complicated to explain simply with a few markers. Besides, a recent report showed that $CCR2^{+}$ inflammatory monocytes are also detected at early time point after ICH (Hammond et al., 2014). In this study, I focused on a considerable increase of Arginase-1 mRNA expression at later time rather than how M1 specific genes are regualted. Further analysis using flow cytometry suggest that macrophages are more likely to defferentiated toward M2 than microglia (Fig. 4). After ICH, CD206, an M2 marker, expression on $CD11b^{+}CD45^{high}$ macrophages significantly increased at later time point, which means that infiltrating macrophages are activated toward M2. This data suggest that recruited macrophages are required in recovery from ICH induced injury by M2 polarization.

A previous study suggests that astrocyte and neuron can induce M2 activation of BMDM via the upregulation of mir-124 (Ponomarev et al., 2011). This show that brain microenvironment may affect macrophage polarization. It is well known that glial cells are the most abundant in the brain. Accordingly, I hypothesized that glial cells in mice brain drive the infiltrating macrophages to the M2 subset. In my study, MBMG induced the M2 polarization of BMDM via soluble factors (Fig. 5, 6). Especially, neurons have a potential to regulate macrophage polarization. The proposed

sources of a signal for M2 phenotype from neurons are various: TGF-β (Bottner et al., 2000), CD200 (Hoek et al., 2000), CX3CL1 (Cardona et al., 2006), Notch1 (Singla et al., 2014), fragmented myelin (Kroner et al., 2014). Based on these studies, it is still possible that neurons also contribute to the macrophage M2 polarization after ICH.

In conclusion, I found that the glial cells-derived factor mediated-M2 activated infiltrating macrophages play a role of repair from ICH.

Ⅴ. REFERENCES

Aronowski J, Hall CE (2005) New horizons for primary intracerebral hemorrhage treatment: experience from preclinical studies. Neurological research 27:268-279.

Bottner M, Krieglstein K, Unsicker K (2000) The transforming growth factor-betas: structure, signaling, and roles in nervous system development and functions. Journal of neurochemistry 75:2227-2240.

Cardona AE, Pioro EP, Sasse ME, Kostenko V, Cardona SM, Dijkstra IM, Huang D, Kidd G, Dombrowski S, Dutta R, Lee JC, Cook DN, Jung S, Lira SA, Littman DR, Ransohoff RM (2006) Control of microglial neurotoxicity by the fractalkine receptor. Nature neuroscience 9:917-924.

Cho IH, Hong J, Suh EC, Kim JH, Lee H, Lee JE, Lee S, Kim CH, Kim DW, Jo EK, Lee KE, Karin M, Lee SJ (2008) Role of microglial IKKbeta in kainic acid-induced hippocampal neuronal cell death. Brain 131:3019-3033.

Ding AH, Nathan CF, Stuehr DJ (1988) Release of reactive nitrogen intermediates and reactive oxygen intermediates from mouse peritoneal macrophages. Comparison of activating cytokines and evidence for independent production. Journal of immunology 141:2407-2412.

Ekdahl CT, Claasen JH, Bonde S, Kokaia Z, Lindvall O (2003) Inflammation is detrimental for neurogenesis in adult brain. Proceedings of the National Academy of Sciences of the United States of America 100:13632-13637.

Gao Z, Wang J, Thiex R, Rogove AD, Heppner FL, Tsirka SE (2008) Microglial activation and intracerebral hemorrhage. Acta neurochirurgica Supplement 105:51-53.

Hammond MD, Ai Y, Sansing LH (2012) Gr1+ Macrophages and Dendritic Cells

Dominate the Inflammatory Infiltrate 12 Hours After Experimental Intracerebral Hemorrhage. Translational stroke research 3:s125-s131.

Hammond MD, Taylor RA, Mullen MT, Ai Y, Aguila HL, Mack M, Kasner SE, McCullough LD, Sansing LH (2014) CCR2+ Ly6C(hi) inflammatory monocyte recruitment exacerbates acute disability following intracerebral hemorrhage. The Journal of neuroscience 34:3901-3909.

Hanisch UK, Kettenmann H (2007) Microglia: active sensor and versatile effector cells in the normal and pathologic brain. Nature neuroscience 10:1387-1394.

Hoek RM, Ruuls SR, Murphy CA, Wright GJ, Goddard R, Zurawski SM, Blom B, Homola ME, Streit WJ, Brown MH, Barclay AN, Sedgwick JD (2000) Down-regulation of the macrophage lineage through interaction with OX2 (CD200). Science 290:1768-1771.

Hu X, Leak RK, Shi Y, Suenaga J, Gao Y, Zheng P, Chen J (2014) Microglial and macrophage polarization-new prospects for brain repair. Nature reviews Neurology.

Hu X, Li P, Guo Y, Wang H, Leak RK, Chen S, Gao Y, Chen J (2012) Microglia/macrophage polarization dynamics reveal novel mechanism of injury expansion after focal cerebral ischemia. Stroke 43:3063-3070.

Joice SL, Mydeen F, Couraud PO, Weksler BB, Romero IA, Fraser PA, Easton AS (2009) Modulation of blood-brain barrier permeability by neutrophils: in vitro and in vivo studies. Brain research 1298:13-23.

Kigerl KA, Gensel JC, Ankeny DP, Alexander JK, Donnelly DJ, Popovich PG (2009) Identification of two distinct macrophage subsets with divergent effects causing either neurotoxicity or regeneration in the injured mouse spinal cord. The Journal of neuroscience 29:13435-13444.

Kroner A, Greenhalgh AD, Zarruk JG, Passos Dos Santos R, Gaestel M, David S

(2014) TNF and increased intracellular iron alter macrophage polarization to a detrimental M1 phenotype in the injured spinal cord. Neuron 83:1098-1116.

Lee SJ, Zhou T, Choi C, Wang Z, Benveniste EN (2000) Differential regulation and function of Fas expression on glial cells. J Immunol 164:1277-1285.

Liu Z, Fan Y, Won SJ, Neumann M, Hu D, Zhou L, Weinstein PR, Liu J (2007) Chronic treatment with minocycline preserves adult new neurons and reduces functional impairment after focal cerebral ischemia. Stroke 38:146-152.

Livak KJ, Schmittgen TD (2001) Analysis of relative gene expression data using real-time quantitative PCR and the 2(-Delta Delta C(T)) Method. Methods 25:402-408.

Marim FM, Silveira TN, Lima DS, Jr., Zamboni DS (2010) A method for generation of bone marrow-derived macrophages from cryopreserved mouse bone marrow cells. PloS one 5:e15263.

Mayer SA, Rincon F (2005) Treatment of intracerebral haemorrhage. The Lancet Neurology 4:662-672.

Miron VE, Boyd A, Zhao JW, Yuen TJ, Ruckh JM, Shadrach JL, van Wijngaarden P, Wagers AJ, Williams A, Franklin RJ, ffrench-Constant C (2013) M2 microglia and macrophages drive oligodendrocyte differentiation during CNS remyelination. Nature neuroscience 16:1211-1218.

Nguyen HX, O'Barr TJ, Anderson AJ (2007) Polymorphonuclear leukocytes promote neurotoxicity through release of matrix metalloproteinases, reactive oxygen species, and TNF-alpha. Journal of neurochemistry 102:900-912.

Perry VH, Nicoll JA, Holmes C (2010) Microglia in neurodegenerative disease. Nature reviews Neurology 6:193-201.

Ponomarev ED, Veremeyko T, Barteneva N, Krichevsky AM, Weiner HL (2011) MicroRNA-124 promotes microglia quiescence and suppresses EAE by deactivating

macrophages via the C/EBP-alpha-PU.1 pathway. Nature medicine 17:64-70.

Shechter R, London A, Varol C, Raposo C, Cusimano M, Yovel G, Rolls A, Mack M, Pluchino S, Martino G, Jung S, Schwartz M (2009) Infiltrating blood-derived macrophages are vital cells playing an anti-inflammatory role in recovery from spinal cord injury in mice. PLoS medicine 6:e1000113.

Sica A, Schioppa T, Mantovani A, Allavena P (2006) Tumour-associated macrophages are a distinct M2 polarised population promoting tumour progression: potential targets of anti-cancer therapy. European journal of cancer 42:717-727.

Singla RD, Wang J, Singla DK (2014) Regulation of Notch1 Signaling in THP-1 Cells Enhances M2 Macrophage Differentiation. American journal of physiology Heart and circulatory physiology:ajpheart 00896 02013.

Wang J, Tsirka SE (2005) Contribution of extracellular proteolysis and microglia to intracerebral hemorrhage. Neurocritical care 3:77-85.

Wang J, Dore S (2007) Inflammation after intracerebral hemorrhage. Journal of cerebral blood flow and metabolism 27:894-908.

Ⅵ. 국문초록

뇌내출혈 (ICH)은 뇌졸중의 중요한 요인 중 하나로서, 전체 뇌졸중 사례에서 약 10%를 차지한다. 대식세포는 활성화되는 방식에 따라 그 종류가 나눠질 수 있다는 것이 잘 알려져 있다. M1 또는 "고전적 활성화" 대식세포는 주로 염증반응을 일으키는 반면, M2 또는 "대체적 활성화" 대식세포의 경우에는 조직을 손상으로부터 회복시키거나 재구성하는 역할을 한다. 마우스 뇌내출혈 모델에서 혈관으로부터 뇌 내로 들어오는 대식세포의 역할과 그 활성화 양상은 아직까지 잘 밝혀져 있지 않기 때문에, 마우스 뇌내출혈 후 그 뇌 내 영역으로 들어오는 대식세포의 표현형과 기능을 연구하였다. 우선 마우스 뇌내출혈을 유도 후 시간이 지남에 따라 혈종 주변영역으로 유입된 대식세포들의 숫자가 증가하고 모여드는 양상을 확인 할 수 있었다. 클로드로네이트 리포좀을 마우스에 복강주사하여 말초의 단핵세포 및 대식세포를 고갈시키는 실험을 통해서, 대조군 마우스에 비해서 말초대식세포가 고갈된 마우스에서 뇌내출혈 후 조직의 손상정도가 더 심하며 행동학적으로도 더 악화된 증상이 나타난다는 것을 밝혔다. 이것은 혈관으로부터 유입되어 들어온 대식세포가 뇌내출혈로부터 회복에 잠정적 역할을 할 수 있음을 시사한다. 그리고 뇌내출혈이 일어난 쪽 뇌반구 조직에서 arginase-1 mRNA (M2 표지자) 의 양은 증가하지만, iNOS mRNA (M1 표지자) 의 양은 통계학적으로 차이가 없었다. 이에 따라 유세포분석기를 이용하여, 같은 방식으로 얻은 뇌조직에서 어떠한 세포에서 M2 활성화가 되는지 확인하였다. 그 결과 만노스수용체 (M2

표지자)를 발현하는 대식세포가 뇌내출혈 후 더 지연된 시간대에서 많이 증가하는 것을 알 수 있었다. 뇌 내로 들어온 대식세포가 M2 활성화 되는 기작에 대해서 대식세포주변 뇌조직 환경이 대식세포의 활성화에 영향을 줄 수 있을 가능성을 예상할 수 있다. 이 가능성을 연구하기 위해서 마우스 골수유래 대식세포와 마우스 혼합뇌교세포를 각각 따로 배양한 뒤 공생배양하여 대식세포의 활성화 타입을 확인하는 실험을 하였다. 뇌교세포와 공생배양하면 만노스수용체를 발현하는 대식세포의 수가 증가하였다. 이 결과는 뇌 내에 가장 많이 존재하는 세포인 뇌교세포가 대식세포의 M2 활성화를 유도할 수 있다는 것을 보여준다. 더욱이, 뇌교세포의 조정배지를 대식세포에 처리해주면 만노스수용체 발현하는 대식세포의 수가 증가하였는데, 이는 뇌교세포로 부터 유래된 수용성 인자가 대식세포의 M2 활성화에 연관되어 있다는 것을 보여준다. 결론적으로, 이 연구결과는 혈관을 순환하던 단핵세포가 뇌내출혈 후 뇌 내로 유입되고 뇌교세포에 의해서 M2 활성화 된 뒤 이것이 뇌내출혈의 손상으로부터 회복하는데 관여한다는 것을 제시한다.

주요어:

뇌내출혈, 뇌졸중, 대식세포, M2 활성화, 골수유래대식세포, 뇌교세포, 클로드로네이트 리포좀